VOL. 11, NO. 10, MAY 2016 ISSN 1819-6608
ARPN Journal of Engineering and Applied Sciences

www.arpnjournals.com

BANK OF KALMAN FILTERS FOR FAULT DETECTION IN QUADROTOR MAV

Dwi Pebrianti[1], Rosdiyana Samad[1], Mahfuzah Mustafa[1], Nor Rul Hasma Abdullah[1] and Luhur Bayuaji[2]
[1]Faculty of Electrical and Electronics Engineering, University Malaysia Pahang, Pekan Campus, Pahang, Malaysia
[2]Faculty of Computer Science and Software Engineering, University Malaysia Pahang, Gambang Campus, Pahang, Malaysia
E-Mail: dwipebrianti@ump.edu.my

ABSTRACT

Fault Detection and Identification (FDI) is a subfield of control engineering which concerns with self-monitoring system, identifying and pinpointing the type and location of failures. This study proposes the application of Kalman Filter for fault detection in quad rotor type MAV. It begins with the development of model of quad rotor, based on rigid body dynamic. The bank of Kalman filters consists of six filters that are associated with the total number of the degree of freedom of the quad rotor. The performance of the fault detection is conducted by simulation using Simulink, Matlab. The result shows that the developed bank of Kalman filters has good performance in detecting a sensor failure during a hovering condition.

Keywords: fault detection and isolation, kalman filter, quad rotor, micro aerial vehicle.

1. INTRODUCTION

Quad rotor Micro Aerial Vehicle (MAV) is one of examples of complex systems that are available in recent technology. MAV has broad application ranging from military and reconnaissance, terrain and utilities inspection, disaster monitoring, environmental surveillance, search and rescue, law enforcement and traffic surveillance, communication relay, media service and remote sensing, etc. [1].

There are a huge number of sensors and actuators inside the quad rotor MAV in order to ensure the given tasks done completely. The more complicated the system is, the maintenance and the control become sophisticated. Once a sensor or actuator prone to failure, it will give effect to the whole process of the system. There is a need that the system could do self-monitoring, identifying when a fault has occurred and pinpointing the type of fault and its location. This capability is usually called as a fault detection and isolation [2].

There are two tasks inside the Fault Detection and Identification (FDI) process which are residual generation and decision making. Residual generation is the process to generate the differences between the ideal model and the actual performance of the system. Once the residual is known, then another sub-system will decide whether the system happens to failures or not. The more advance FDI process will also generate the location of the failures.

Frank *et al.* [3] and Hammouri *et al.* [4] use of nonlinear observers for fault detection and isolation. Hammouri *et al.* [5,6] discuss the use of high-gain observers for fault detection of control affine nonlinear systems.

In a stochastic setting to observer-based fault detection, Alessandri *et al.* [7] used extended Kalman filter (EKF) for detection of actuator faults in unmanned underwater vehicles. Wei *et al.* developed a bank of Kalman filters to conduct fault diagnosis of aircraft engine sensor or actuator.

From the works, it can be concluded that the accuracy of the model has direct impact on diagnostic system performance and reliability. In other words, the more accurate the model, the more reliable will be the model-based fault diagnosis scheme. However, for complex and uncertain systems, the derivation of high-fidelity mathematical models from physical principles can become very complicated, time consuming, and even sometimes unfeasible. Moreover, even with the possibility of deriving a mathematical model using first principles, obtaining accurate model parameter values may become a very tedious job or even practically impossible due to proprietary issues regularly imposed by system integrators. Additionally, some systems exhibit uncertain behaviors such as higher order dynamics and high-frequency oscillations, collectively called unmodeled dynamics, which cannot be precisely modeled.

The second approach is computational intelligence based FDI such as neural networks, fuzzy-logic, neuro-fuzzy systems, and genetic algorithms. This technique represents a promising way of circumventing the above-mentioned modeling precision problems in model-based fault diagnosis. The works on computational intelligence based FDI can be found in references [8] – [12]. From the literatures, mostly they consider the plant as a linear system. Generally, a linearization method is applied when they deal with nonlinear system. This approach may lead to the unrobustness of the system.

The Computer Intelligence (CI)-based diagnostic methods use either qualitative or quantitative information about a system in order to achieve fault diagnosis. Both methodologies have been successfully applied to fault diagnosis of various engineering systems; however, integrating both quantitative and qualitative information can greatly enhance the diagnostic system performance and robustness.

In this paper, the diagnosis of sensor faults in a quad rotor MAV is investigated and the design of a fault detection system is considered, using a model-based

approach. The dynamic models developed for the quad rotor are illustrated in Section 2. In Section 3, a bank Kalman filter that will be used for the residual generation is considered, to describe the dynamics of the vehicle with the sensor faults. The fault-detection scheme, based on a bank of KFs will be also discussed. The results of the simulation on the proposed algorithm will be discussed in Sections 4. Section 5 will be the conclusion and future works.

2. MATHEMATICAL MODEL OF QUAD ROTOR MAV

a) Rigid body dynamics

Modeling the rigid body dynamics aims at finding the differential equations that relate system outputs (position and orientation) to its inputs (force and torque vectors). The equations of motion for a rigid body subject to external force $F^{ext} \in R^3$ and torque vector $\Gamma^b \in R^3$ is given by the following Newton – Euler equations, expressed in the body-fixed reference frame $\boldsymbol{B}$.

$$\begin{aligned} m\dot{V} + \Omega \times mV &= F \\ J\dot{\Omega} + \Omega \times J\Omega &= \Gamma^b \end{aligned} \tag{1}$$

where $V = (u, v, w)$ and $\Omega = (p, q, r)$ are respectively, the linear and angular velocities in the body-fixed reference frame. The translation force Fcombines gravity, main thrust and other body force components.

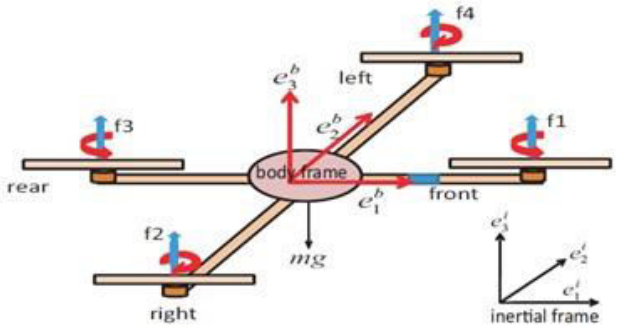

Figure-1. Rigid body dynamics and associated frames [1].

Using Euler angles parameterization and "ZYX" convention, the airframe orientation in space is given by a rotation matrix R from $\boldsymbol{B}$ to the inertial reference frame $\boldsymbol{I}$, where $R \in SO3$ is expressed as follows:

$$\begin{aligned} R &= R_\psi \cdot R_\theta \cdot R_\varphi \\ &= \begin{bmatrix} c\theta c\psi & s\phi s\theta c\psi - c\phi s\psi & c\phi s\theta c\psi + s\phi s\psi \\ c\theta s\psi & s\phi s\theta s\psi + c\phi c\psi & c\phi s\theta s\psi - s\phi c\psi \\ -s\theta & s\phi c\theta & c\phi c\theta \end{bmatrix} \end{aligned} \tag{2}$$

where $\eta = (\phi, \theta, \psi)$ denotes the vector of three Euler angles and s., c. are abbreviation for sin(.) and cos(.).

By considering this transformation between the body-fixed reference frame $\boldsymbol{B}$ and the inertia reference frame $\boldsymbol{I}$ as seen in Figure-1, it is possible to separate the gravitational force from other forces and write the translation dynamics in I as follows:

$$\begin{aligned} \dot{\xi} &= v \\ m\dot{v} &= RF^b - mge_3^i \end{aligned} \tag{3}$$

where $\xi = (x, y, z)$ and $v = (\dot{x}, \dot{y}, \dot{z})$ are the quad-rotor position and velocity in $\boldsymbol{I}$. g is the gravitational acceleration and F^b is the resulting force vector in $\boldsymbol{B}$ (excluding the gravity force) acting on the airframe.

In this research, we used Euler angle parameterization to express rotational dynamics in an appropriate form for control design. The kinematic relation between is expressed by using Equation.4 written below.

$$\dot{\eta} = \Phi(\eta)\Omega \tag{4}$$

where the Euler matrix $\Phi(\eta)$ is given by

$$\Phi(\eta) = \begin{bmatrix} 1 & \sin(\phi)\tan(\theta) & \cos(\phi)\tan(\theta) \\ 0 & \cos(\phi) & -\sin(\theta) \\ 0 & -\sin(\phi) & \cos(\phi)\sec(\theta) \end{bmatrix} \tag{5}$$

It is important to note that the matrix Φ has a singularity at $\theta = \pm\pi/2$, and its inverse matrix $\Psi(\eta) = \Phi^{-1}(\eta)$ is given by

$$\Psi(\eta) = \begin{bmatrix} 1 & 0 & -\sin(\theta) \\ 0 & \cos(\phi) & \cos(\theta)\sin(\phi) \\ 0 & -\sin(\phi) & \cos(\theta)\cos(\phi) \end{bmatrix} \tag{6}$$

By differentiating Equation.4 with respect to time, and recalling the second equation Equation.1, we write

$$\ddot{\eta} = \dot{\Phi}\Omega + \Phi\dot{\Omega} = \dot{\Phi}\Psi\dot{\eta} - \Phi J^{-1}sk(\Omega)J\Omega + \Phi J^{-1}\Gamma^b \tag{7}$$

The *sk* operation is defined here from $\boldsymbol{R}^3$ to $\boldsymbol{R}^{3\times3}$ such that $sk(x)$ is a skew-symmetric matrix associated to the vector product $sk(x)y \coloneqq x \times y$ for any vector$y \in \boldsymbol{R}^3$.

By multiplying both sides of the last equation by $M(\eta) = \Psi(\eta)^T J\Psi(\eta)$, we obtain

$$M(\eta)\ddot{\eta} + C(\eta, \dot{\eta}) = \Psi(\eta)\Gamma^b \tag{8}$$

with $M(\eta)$ is a well defined positive inertia matrix, provided that $\theta \neq k\pi/2$. The *Coriolis* term $C(\eta, \dot{\eta})$ is given by

$$C(\eta, \dot{\eta}) = -\Psi(\eta)^T J\Psi(\eta) + \Psi(\eta)^T sk(\Psi(\eta)\dot{\eta})J\Psi(\eta) \tag{9}$$

Thus, the quad-rotor nonlinear model, used for flight controller design, is

$$m\ddot{\xi} = RF^b - mge_3^i$$
$$M(\eta)\ddot{\eta} + C(\eta,\dot{\eta})\dot{\eta} = \Psi(\eta)^T\Gamma^b \quad (10)$$

b) Aerodynamics forces and torques

Quad-rotor MAV can be characterized by three main control torques $\tau = (\tau_\phi, \tau_\theta, \tau_\psi)^T$ and one main control force $F^b = (0,0,u)^T$. The four control inputs $(u, \tau_\phi, \tau_\theta, \tau_\psi)$ are obtained by independently controlling the rotation speed of each motor. The collective lift u is the sum of the thrusts generated by the four propellers.

$$u = \sum_{i=1}^{4} f_i \quad (11)$$

The airframe torques generated by rotors are given by [13].

$$\tau_\phi = l(f_2 - f_4)$$
$$\tau_\theta = l(f_3 - f_1)$$
$$\tau_\psi = Q_1 + Q_3 - Q_2 - Q_4 \quad (12)$$

l represents the distance from the rotors to the center of mass of the helicopter and Q_i is the fan torque due to air drag.

Propellers thrust and torque are generally assumed to be proportional to the square of the rotor angular velocity ω. In fact, the relations between the rotor speed w_i and the generated lift f_i and torque Q_i are very complex.[14] Therefore, the algebraic model for generating the force and control torques can be written in the following form:

$$\begin{bmatrix} u \\ \tau_\phi \\ \tau_\theta \\ \tau_\psi \end{bmatrix} = \begin{bmatrix} \rho & \rho & \rho & \rho \\ 0 & -l\rho & 0 & l\rho \\ -l\rho & 0 & l\rho & 0 \\ k & -k & k & -k \end{bmatrix} \begin{bmatrix} w_1^2 \\ w_2^2 \\ w_3^2 \\ w_4^2 \end{bmatrix} \quad (13)$$

Where (ρ, k) are positive constants characterizing the propellers aerodynamics. The expressions in Equation.13 are valid approximations that are used in cases of hovering and low-speed displacements.

The dynamical model, considered for quad-rotor control design is given by the following Equation.14:

$$m\ddot{\xi} = uRe_3^i - mge_3^i$$
$$M(\eta)\ddot{\eta} + C(\eta,\dot{\eta})\dot{\eta} = \Psi(\eta)^T\tau \quad (14)$$

3. SENSOR FAULT MODELLING

This study is limited to actuator fault detection. In order to describe the fault model of the vehicle, a brief understanding regarding the controller designed is needed. In this case, the controller used is PID controller. As mentioned in Section 2, quad rotor system has four inputs and six outputs. It has inner loop for controlling the attitude and outer loop for controlling the position of the quad rotor. The desired attitude is $\eta_d = (\phi_d, \theta_d, \psi_d)$. The desired position is $\xi_d = (x_d, y_d, z_d)$. The block diagram of the system with the PID controller is shown in Figure-2.

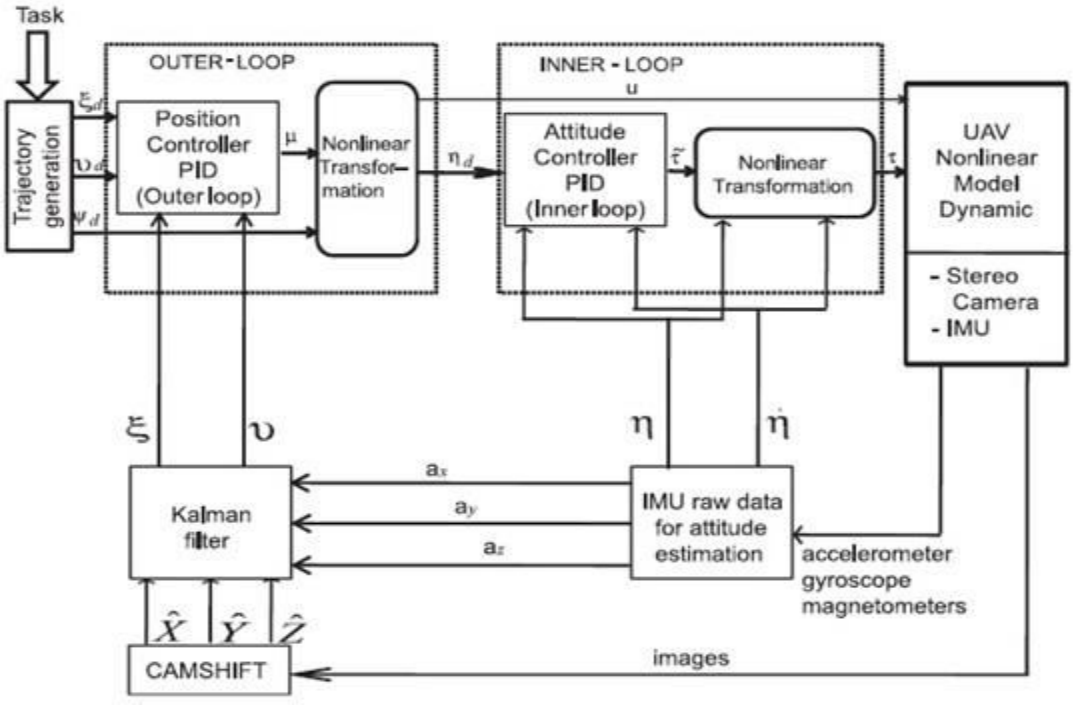

Figure-2. Block diagram of quad rotor with PID controller. [1].

The values of PID gain for attitude and position controller are concluded in Table-1. More detail explanation regarding the controller design can be found in [1].

Table-1. Controller gain.

Parameters	Values	Parameters	Values
k_{px}, k_{py}	0.8	$k_{p\phi}, k_{p\theta}$	28.0
k_{ix}, k_{iy}	0.02	$k_{i\phi}, k_{i\theta}$	0.5
k_{dx}, k_{dy}	1.0	$k_{d\phi}, k_{d\theta}$	1.0
k_{pz}	0.2	$k_{p\psi}$	3.0
k_{iz}	0.02	$k_{i\psi}$	0.05
k_{dz}	0.6	$k_{d\psi}$	0.2

Since model used in this study is non-linear model, there is a need to do linearization in order to design the Kalman Filter (KF) for the sensor fault detection task. The linearization process was conducted for hovering state, where quad rotor is flying in a static condition. The vector of $\xi = (x, y, z) = (0,0,0)$, $v = (\dot{x}, \dot{y}, \dot{z}) = (0,0,0)$ $\eta = (\phi, \theta, \psi) = (0,0,0)$ and $\dot{\eta} = (\dot{\phi}, \dot{\theta}, \dot{\psi}) = (0,0,0)$.

Generally, a linear system can be represented with the matrix written below.

$$\dot{x} = Ax + Bu$$
$$y = Cx + Du \quad (15)$$

To obtain linear state space representation, non-linear system in Equation.14 is derived as follows:

$$A = \begin{bmatrix} \frac{df_1}{dx_1} & \cdots & \frac{df_1}{dx_{12}} \\ \vdots & & \vdots \\ \frac{df_{12}}{dx_1} & \cdots & \frac{df_{12}}{dx_{12}} \end{bmatrix} \quad (16)$$

$$B = \begin{bmatrix} \frac{df_1}{dU_1} & \cdots & \frac{df_1}{dU_4} \\ \vdots & & \vdots \\ \frac{df_{12}}{dU_1} & \cdots & \frac{df_{12}}{dU_4} \end{bmatrix} \quad (17)$$

Thus, linear system state space that can be applied to design the Kalman Filter is obtained as shown in Equation. 18 and Equation.19.

$$A = \begin{bmatrix} 0 & 1 & 0 & 0 & 0 & 0 & 0 & 0 & 0 & 0 & 0 & 0 \\ 0 & 0 & 0 & 0 & 0 & 0 & 0 & 0 & -g & 0 & 0 & 0 \\ 0 & 0 & 0 & 1 & 0 & 0 & 0 & 0 & 0 & 0 & 0 & 0 \\ 0 & 0 & 0 & 0 & 0 & 0 & g & 0 & 0 & 0 & 0 & 0 \\ 0 & 0 & 0 & 0 & 0 & 1 & 0 & 0 & 0 & 0 & 0 & 0 \\ 0 & 0 & 0 & 0 & 0 & 0 & 0 & 0 & 0 & 0 & 0 & 0 \\ 0 & 0 & 0 & 0 & 0 & 0 & 0 & 1 & 0 & 0 & 0 & 0 \\ 0 & 0 & 0 & 0 & 0 & 0 & 0 & 0 & 0 & 0 & 0 & 0 \\ 0 & 0 & 0 & 0 & 0 & 0 & 0 & 0 & 0 & 1 & 0 & 0 \\ 0 & 0 & 0 & 0 & 0 & 0 & 0 & 0 & 0 & 0 & 0 & 0 \\ 0 & 0 & 0 & 0 & 0 & 0 & 0 & 0 & 0 & 0 & 0 & 1 \\ 0 & 0 & 0 & 0 & 0 & 0 & 0 & 0 & 0 & 0 & 0 & 0 \end{bmatrix} \quad (18)$$

$$B = \begin{bmatrix} 0 & 0 & 0 & 0 \\ 0 & 0 & 0 & 0 \\ 0 & 0 & 0 & 0 \\ 0 & 0 & 0 & 0 \\ 0 & 0 & 0 & 0 \\ \frac{1}{m} & 0 & 0 & 0 \\ 0 & 0 & 0 & 0 \\ 0 & \frac{l}{Ix} & 0 & 0 \\ 0 & 0 & 0 & 0 \\ 0 & 0 & \frac{l}{Iy} & 0 \\ 0 & 0 & 0 & 0 \\ 0 & 0 & 0 & \frac{l}{Iz} \end{bmatrix} \quad (19)$$

The fault detection problem is formulated as a min-max problem by generalizing the least-square derivation of the Kalman filter.

a) Fault detection using Kalman filter

The Kalman filter is designed for the normal fault-free operation. The model of the system for a fault-free is the one after linearized as mention in previous section. The equation can be rewrite as follow.

$$x(k+1) = A_0 x(k) + B_0 u(k-d) + w(k)$$
$$y(k) = C_0 x(k) + v(k) \quad (20)$$

where $y(k)$ is the output, in this case quad rotor position, $\xi = (x, y, z)$ and quad rotor attitude $\eta = (\phi, \theta, \psi)$. A_0 is the one in Equation. 18. B_0 is the one in Eq.19. C_0 is matrix that is correlated with the output of the system that can be measured by the sensor. In this case, we define that the output comes from the attitude sensor, roll (ϕ), pitch (θ) and yaw (ψ). It can be written as Equation.21.

$w(k)$ and $v(k)$ are zero mean white plant and measurement noise signals, respectively, with covariances:

$$C = \begin{bmatrix} 1 & 0 & 0 & 0 & 0 & 0 & 0 & 0 & 0 & 0 & 0 & 0 \\ 0 & 0 & 1 & 0 & 0 & 0 & 0 & 0 & 0 & 0 & 0 & 0 \\ 0 & 0 & 0 & 0 & 1 & 0 & 0 & 0 & 0 & 0 & 0 & 0 \\ 0 & 0 & 0 & 0 & 0 & 0 & 1 & 0 & 0 & 0 & 0 & 0 \\ 0 & 0 & 0 & 0 & 0 & 0 & 0 & 0 & 1 & 0 & 0 & 0 \\ 0 & 0 & 0 & 0 & 0 & 0 & 0 & 0 & 0 & 0 & 1 & 0 \end{bmatrix} \quad (21)$$

$w(k)$ and $v(k)$ are zero mean white plant and measurement noise signals, respectively, with covariances:

$$Q = E[w(k)w^T(k)]\ ;\ R = E[v(k)v^t(k)] \quad (22)$$

The plant noise, $w(k)$, is a mathematical artifice introduced to account for the uncertainty in the *a-priori* knowledge of the plant model. The larger the covariance Q is, the less accurate the model (A_0, B_0, C_0) is and vice versa.

The Kalman filter is given by:

$$\hat{x}(k+1) = A_0\hat{x}(k) + B_0u(k-d) + K_0(y(k) - C_0\hat{x}(k))$$
$$e_k = y(k) - C_0\hat{x}(k) \quad (23)$$

where d is the delay and e_k is the residual.

The system model has a pure time delay which is incorporated in the Kalman filter formulation. The Kalman filter estimates the states by fusing the information provided by the measurement $y(k)$ and the *a-priori* information contained in the model, (A_0, B_0, C_0). This fusion is based on the *a priori* information of the plant and the measurement noise covariances, Q, and R, respectively. When Q is small, implying that the model is accurate, the state estimate is obtained by weighting the plant model more than the measurement one. The Kalman gain, K_0, will then be small. On the other hand, when R is small implying that the measurement model is accurate, the state estimate is then obtained by weighting the measurement model more than the plant one. The Kalman gain, K_0, will be large in this case.

The larger $K0$ is, the faster the response of the filter will be and the larger the variance of the estimation error becomes. Thus, there is a trade-off between a fast filter response and a small covariance of the residual. The selection of Kalman filter gain K_0 is conducted empirically.

The overall structure of the fault detection using a bank of Kalman filters is shown in Figure 3. The information regarding 1st sensor until 6th sensor are roll, pitch, yaw, x y and z position, respectively.

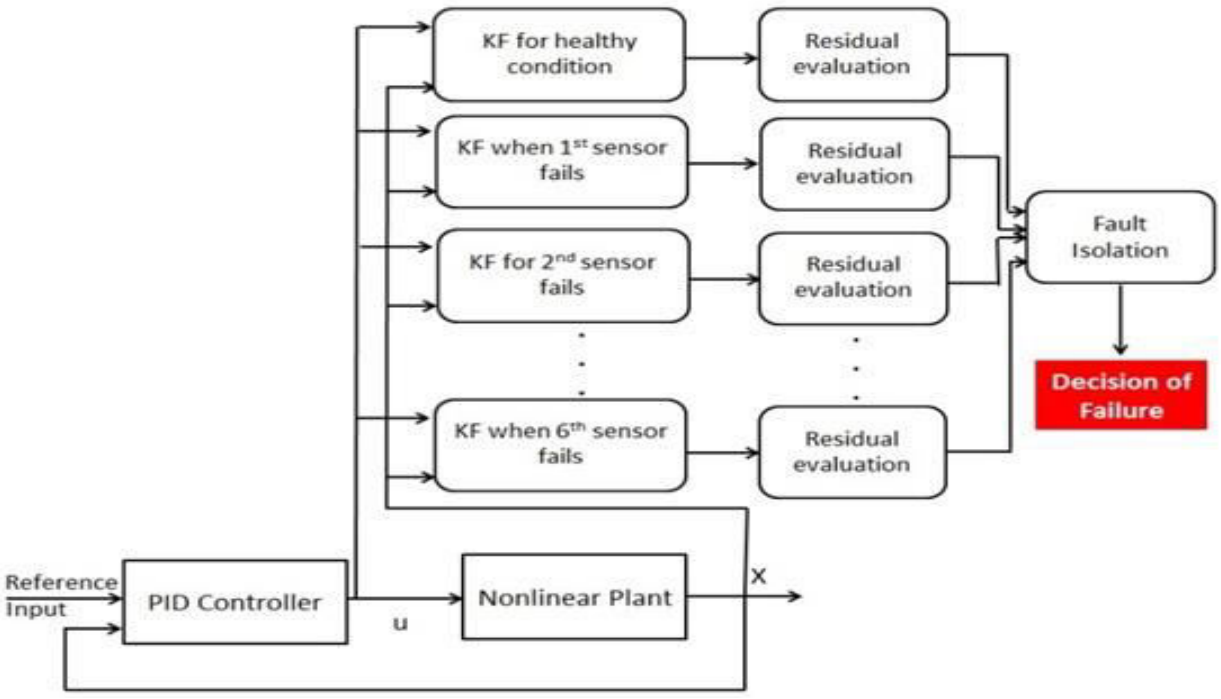

Figure-3. Bank of Kalman filter for fault detection.

4. RESULT AND DISCUSSION

The simulation is conducted under the hovering condition. In hovering condition, the values of all rotor speeds are the same. The desired attitude is $\eta_d = (\phi_d, \theta_d, \psi_d) = (0,0,0)$ and the desired position is $\xi_d = (x_d, y_d, z_d) = (0,0,1)$. This means that the quad rotor is hovering at 1 meter of altitude.

The performance of the bank of Kalman Filter is evaluated in the term of the residual generated. In case of healthy condition, the residual generated will be below of a certain threshold. Once, there is a problem on the sensor measurement, e.g. IMU has problem for detecting the roll, the value of Kalman filter for detecting roll sensor failure will be above the given threshold.

Figure-4 shows the performance of the proposed method. The performance during the normal condition is shown with the solid line. The performance during the sensor failure is shown in dashed line. Here we can see that the proposed Kalman filter is able to detect the sensor failure.

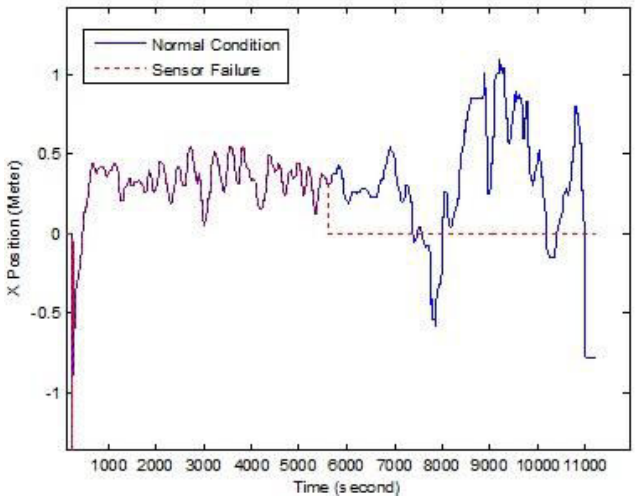

Figure-4. X position measurement.

Figure-5 shows the residual generated. During the normal condition the residual is close to zero. However, when a failure happened, the residual value is suddenly increasing. This feature will be used for the fault identification task.

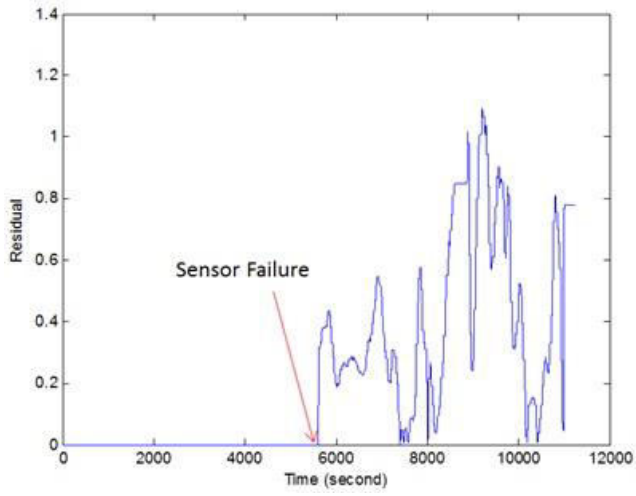

Figure 5. Residual generated with failure on sensor X position.

5. CONCLUSION AND FUTURE WORKS

This study discusses about the application of bank of Kalman filter for the fault detection task in quad rotor MAV. The work is started with the design of mathematical model of the quad rotor based on rigid body dynamics. A linearization process is conducted on the hovering condition. Under the hovering condition, seven Kalman filters stored in bank of Kalman filters are derived. By using this bank of Kalman filters, a fault detection process is conducted. The result shows that the proposed method can detect a failure when IMU sensor failed to measure the roll value.

As the future works, this system will be combined with a Neural Network, in order to build a complete fault detection and isolation system.

ACKNOWLEDGEMENTS

This works is supported by Ministry of Higher Education Malaysia, under the Fundamental Research Grant Scheme, FRGS RDU 140137.

REFERENCES

[1] Dwi Pebrianti, Farid Kendoul, Syaril Azrad, Wei Wang and Kenzo Nonami. 2010. Autonomous Hovering and Landing of a Quad-rotor Micro Aerial Vehicle by Means of on Ground Stereo Vision System. Journal of System Design and Dynamics. 4(2): 269 - 284.

[2] Edwards C., Pin Tan C., Alwi H. 2011. Fault Detection and Fault Tolerant Control Using Sliding Modes. XXVIII, ISBN: 978 – 0 – 85729 – 649 – 8.

[3] P. M. Frank, G. Schrier, E. AlcortaGarcía. 1999. Nonlinear observers for fault detection and isolation. Lecture Notes in Control and Information Sciences Volume 244: 399-422.

[4] H. Hammouri, M. Kinnaert, and E. H. El Yaagoubi. 1999. Observer-Based Approach to Fault Detection and Isolation for Nonlinear Systems. IEEE Transactions on Automatic Control 44(10).

[5] H. Hammouri, P. Kabore, and M. Kinnaert. 2001. A Geometric Approach to Fault Detection and Isolationfor Bilinear Systems. IEEE Transactions on Automatic Control 46(9).

[6] H. Hammouri, P. Kabore, S. Othman and J. Biston. 2002. Failure Diagnosis and Nonlinear Observer Application to a Hydraulic Process. Journal of the Franklin Institute of the State of Pennsylvania 339(4-5): 455-478.

[7] A. Alessandri*, M. Caccia, G. Veruggio. 1999. Fault detection of actuator faults in unmanned underwater vehicles. Control Engineering Practice 7: 357 – 368.

[8] Rafik Zouari, Sophie Sieg-Zieba, Menad Sidahmed. 2004. Fault Detection System For Centrifugal Pumps Using Neural Networks A

[9] Neuro-Fuzzy Techniques. Proceeding of Surveillance 5 CETIM Senlis.

[10] HesamKomariAlaei, Karim Salahshoor and HamedKomariAlaei. 2013. A new integrated on-line fuzzy clustering and segmentation methodology with adaptive PCA approach for process monitoring and fault detection and diagnosis. Journal of Soft Computing 17: 345–362.

[11] Soheil Bahrampour, Behzad Moshiri and Karim Salahshoor. 2011. Weighted and constrained possibilistic C-means clustering for online fault detection and isolation. Journal of Application Intelligence 35: 269–284.

[12] H. A. Talebi, K. Khorasani, and S. Tafazoli. 2009. A Recurrent Neural-Network-Based Sensor and Actuator Fault Detection and Isolation for Nonlinear Systems with Application to the Satellite's Attitude Control Subsystem. IEEE Transactions on Neural Networks 20(1).

[13] L. Felipe Blazquez, Luis J. de Miguel, Fernando Aller and Jose R. Peran. 2011. Neuro-fuzzy identification applied to fault detection in nonlinear systems. International Journal of Systems Science 42(10): 1771–1787.

[14] P. Castillo, R. Lozano, and A. Dzul. 2005. Modelling and Control of Mini-Flying Machines. Advances in Industrial Control, Springer-Verlag.

[15] F. Kendoul. 2009. Nonlinear Hierarchical Flight Controller for Unmanned Rotorcraft: Design, Stability and Experiments. Engineering Notes, Journal of Guidance, Control and Dynamics.